Electronic Supplementary Information (ESI) for:

Synthesis and thermal stability of ZrO_2@SiO_2 core-shell submicron particles

Maik Finsel,[a] Maria Hemme,[a] Sebastian Döring,[1a] Jil S. V. Rüter,[a] Gregor T. Dahl,[a] Tobias Krekeler,[b] Andreas Kornowski,[a] Martin Ritter,[b] Horst Weller [a] and Tobias Vossmeyer [*a]

[a]*Institute of Physical Chemistry, University of Hamburg, Grindelallee 117, D-20146 Hamburg, Germany. E-mail: tobias.vossmeyer@chemie.uni-hamburg.de*

[b]*Electron Microscopy Unit, Hamburg University of Technology, Eißendorfer Straße 42, D-21073 Hamburg, Germany*

[1] Present address: *AB-Analytik Dr. A. Berg GmbH, Ruhrstraße 49, D-22761 Hamburg, Germany*

TABLE OF CONTENTS

1. PARTICLE SIZES

Fig. S1 presents TEM images and size histograms of as-synthesized (a, b) and calcined (c, d) zirconia particles. The as-synthesized particles had a diameter of 311 nm ± 12%. After synthesis, the particles were first dried at 80 °C for 4 hours and then calcined at 400 °C for 3 hours with a heating ramp of 5 °C/min and with a cooling rate of ≤ 5 °C/min. The calcined particles had a diameter of 273 nm ± 11%.

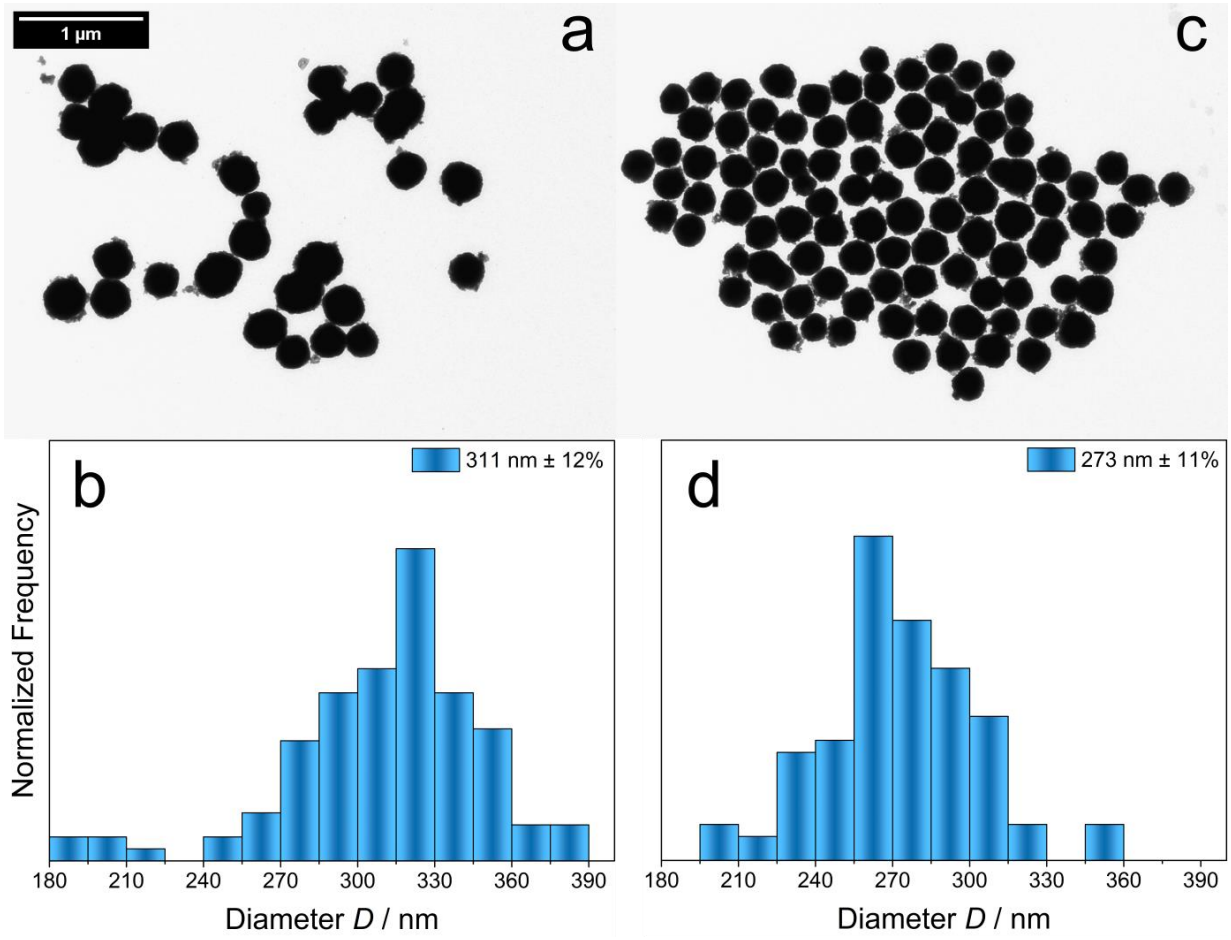

Fig. S1. TEM images and sizing statistics of as-synthesized (a, b) and calcined (c, d) zirconia submicron particles. Average particle diameters and standard deviations were determined using *ImageJ* software by counting at least 100 particles.

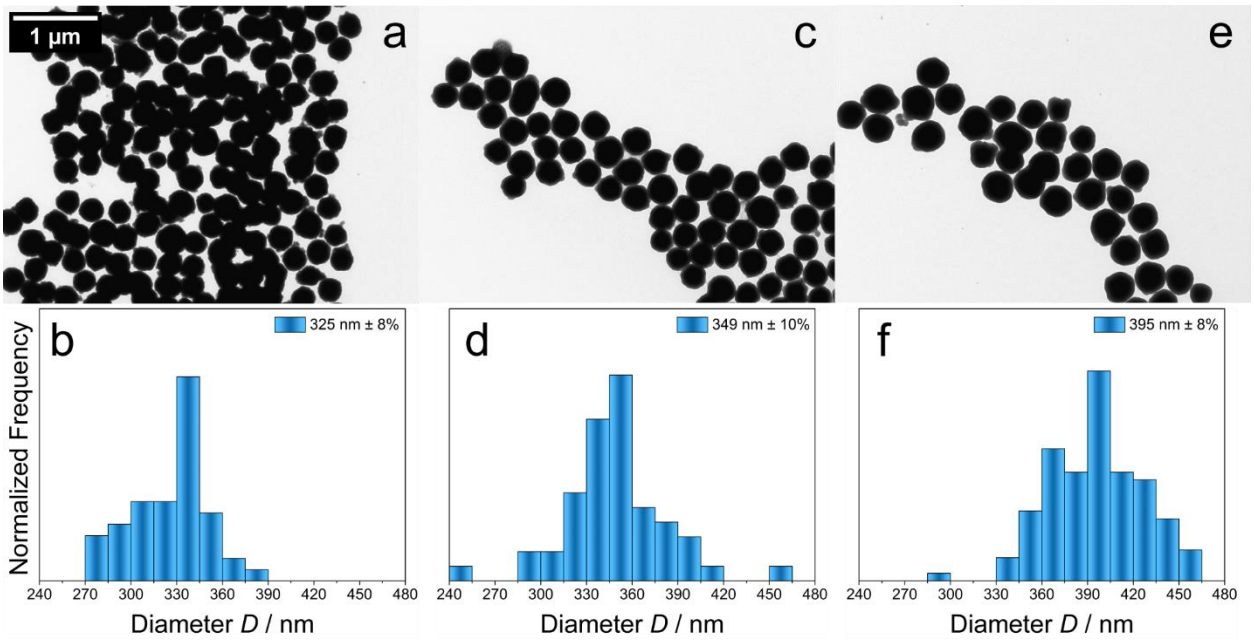

Fig. S2. TEM images and sizing statistics of ZrO_2@SiO_2 particles with different initial silica shell thicknesses (a,b: ~26 nm; c,d: ~38 nm; e,f: ~61 nm). Average particle diameters and standard deviations were determined using *ImageJ* software by counting at least 100 particles.

TEM images and sizing statistics of the silica encapsulated zirconia cores with three different shell thicknesses are presented in Fig. S2. After depositing the silica shells, the particles were isolated and dried at 80 °C for 4 hours, before their sizes were determined by TEM. With increasing shell thickness the average particle sizes were 325 nm ± 12%, 349 nm ± 10%, and 395 nm ± 8%. Subtracting the average core size (273 nm) from the average diameters of the ZrO_2@SiO_2 particles returned silica shell thicknesses of 26, 38, and 61 nm.

2. THERMAL STABILITY

2.1. TGA-DSC

Fig. S3 shows the TGA-DSC curves of the ZrO_2@SiO_2 core-shell particles (initial silica shell thickness: ~38 nm) recorded up to 1200 °C (heating rate: 5 °C/min). Thermogravimetric analysis (TGA, blue curve) revealed a regular mass loss of ~9% whilst heating under an N_2/O_2 atmosphere (gas flow: 30 mL/min). As the zirconia cores were pre-calcined at 400 °C (3 h), the mass loss up to 400 °C mainly originates from loss of water, residual organic precursor, and solvent from the silica shell. The subsequent steeper trend of the TGA curve at higher temperatures is due to loss of residual organics and water from, both, the core and the shell. The DSC curve (black) shows a first exothermic peak between 100 and 850 °C, which we tentatively attribute to the exothermic decomposition (oxidation) of residual organics and the crystallization of the remaining amorphous zirconia phase.[1] A second, smaller exothermic peak between 850 and 1200 °C peak may be attributed to the martensitic $t \rightarrow m$ phase transformation as clearly observed in the XRD data in Fig. 5 (main document).[2]

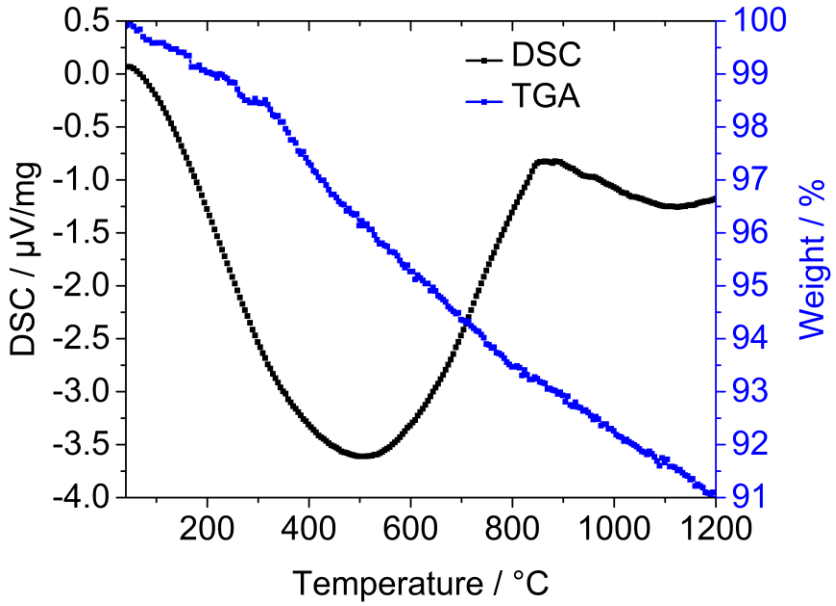

Fig. S3. TGA-DSC curves of the ZrO_2@SiO_2 core-shell particles (initial silica shell thickness: ~38 nm) recorded up to 1200 °C (heating rate: 5 °C/min, air atmosphere).

2.2. Temperature profiles

Fig. S4 shows the temperature profiles used for the calcination of particle samples.

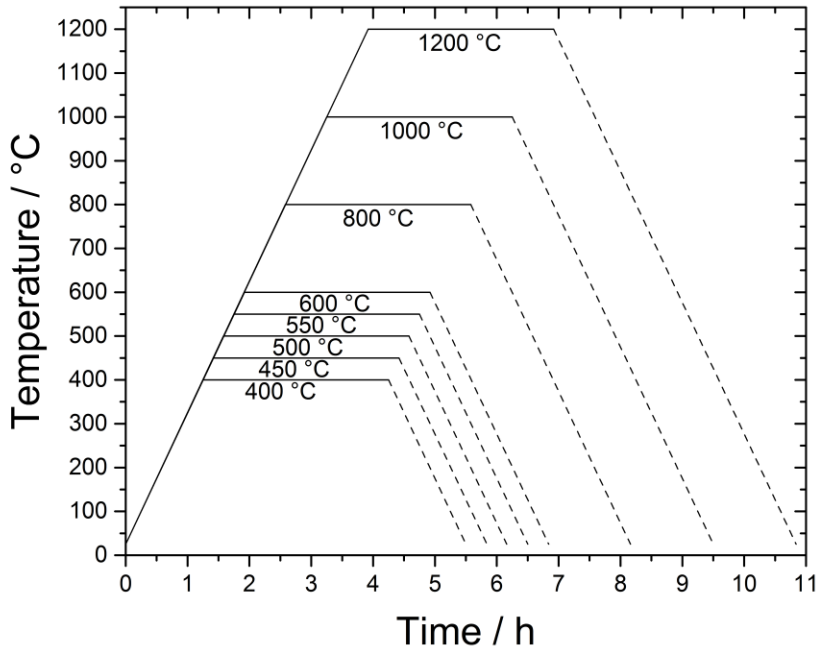

Fig. S4. Temperature profiles used for calcination experiments. The heating rate was 5 °C/min and the highest temperature was kept constant for 3 h. The cooling rate was ≤ 5 °C/min.

2.3. Shape stability

Fig. S5 shows SEM images of bare zirconia cores and ZrO_2@SiO_2 core-shell particles after calcination at different temperatures, as indicated. In the case of the bare zirconia cores significant grain coarsening is observed after calcining at 600 and 800°C, leading to degradation of the original spheroidal particle shape. After heating to 1000 °C the initial particle shape was completely destroyed. The ZrO_2@SiO_2 core-shell particles are shape persistent, even after heating to 1000 °C. The particles with the thinnest shell (initial thickness: ~26 nm) showed a somewhat

higher surface roughness than the other two samples with initial shell thicknesses of ~38 and ~61 nm. After heating to 1200 °C, all particles had lost their original spheroidal shape.

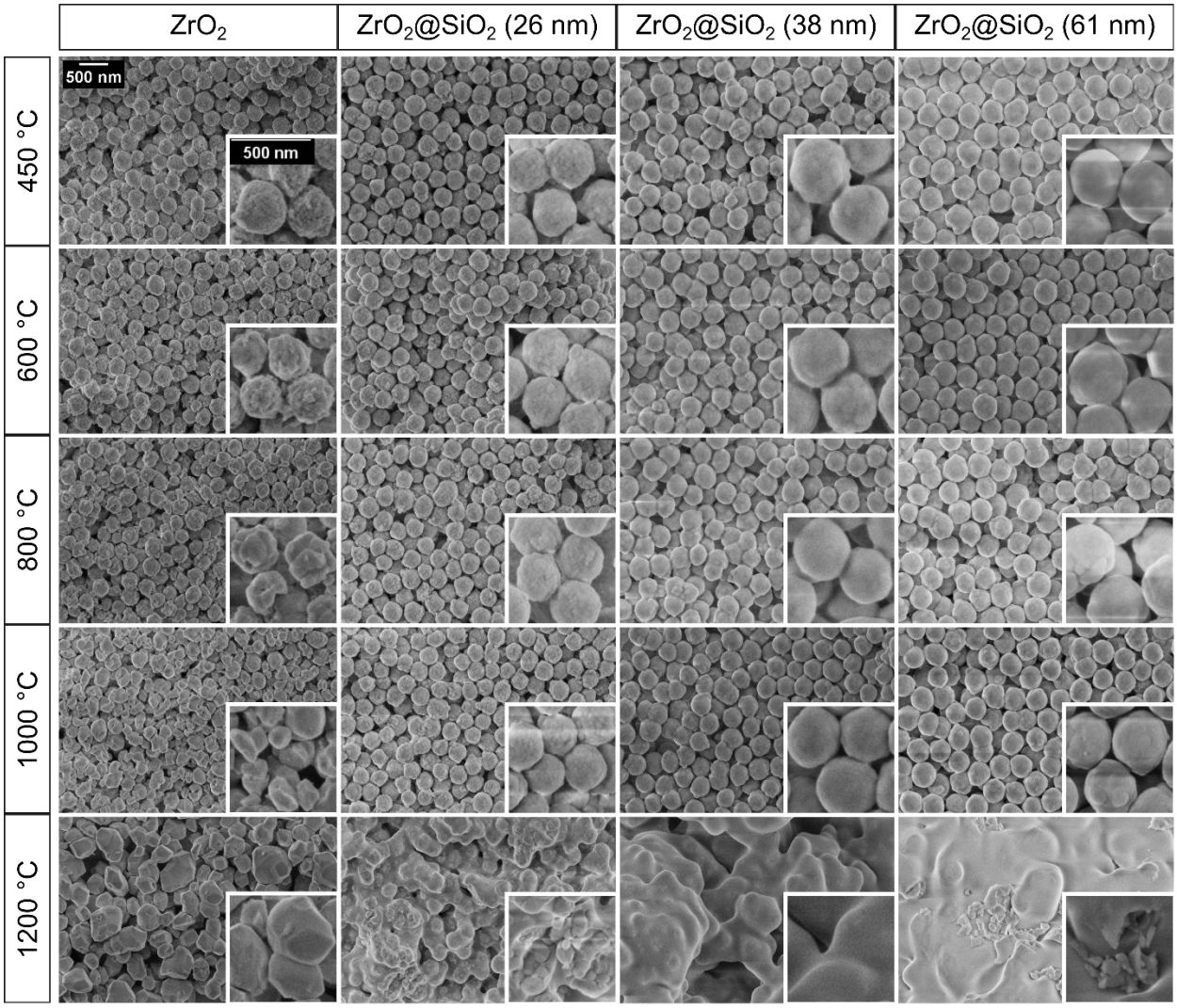

Fig. S5. SEM images of bare ZrO_2 cores and ZrO_2@SiO_2 core-shell particles after 3 h calcination at 450, 600, 800, 1000, and 1200 °C, as indicated.

2.4. Phase stability and grain growth

The crystalline phases of the heat-treated samples were investigated by powder X-ray diffraction using a Philips X'Pert PRO MDP apparatus with Cu-K_α anode and Bragg-Brentano geometry. Single side polished (911)-oriented silicon wafers were used as substrates. Fig. S6(a) shows the XRD data of the bare zirconia core particles after calcination at different temperatures, as indicated. After drying at 80 °C the particles were amorphous. They transitioned mainly to the tetragonal phase after the heat treatment at 400 °C. However, as seen in Fig. 6(b), some crystallites had already transitioned to the monoclinic phase. After further increasing the calcination temperature the tetragonal crystallites gradually transitioned to the monoclinic phase. This transformation was almost complete after calcining at 600 °C and finalized after heating to 800 °C.

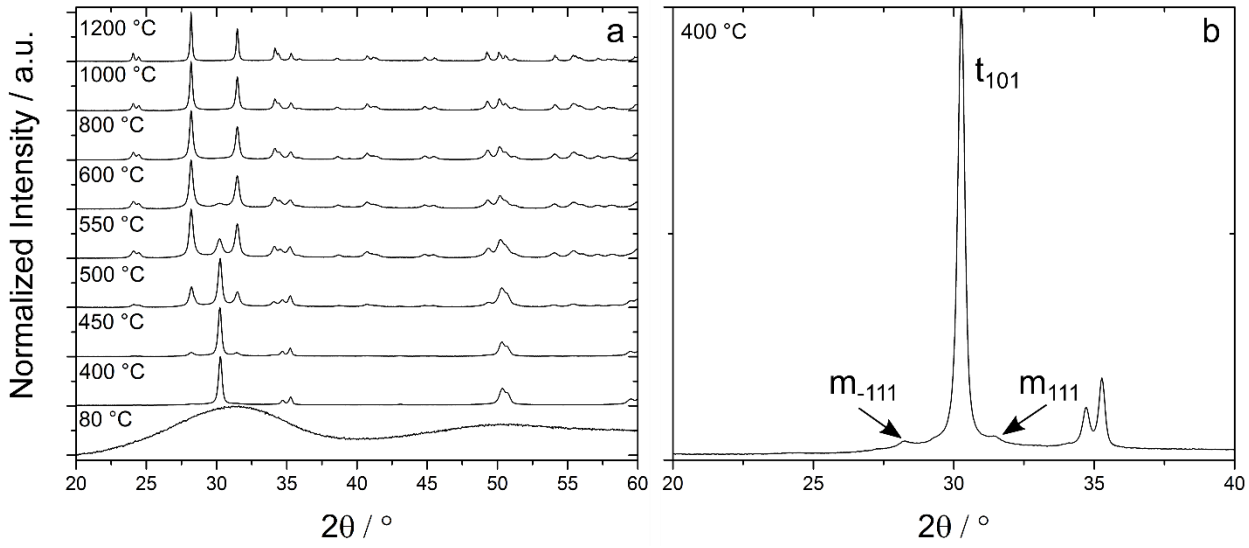

Fig. S6. XRD data of bare zirconia cores acquired after calcination at different temperatures, as indicated. (a). Faint signals of the monoclinic phase are already observed after calcination at 400 °C (b).

Crystallite sizes (grain sizes) were determined from XRD data using the Scherrer equation[3] (Eq. 1). The full width *w* at half maximum (FWHM) was obtained by fitting Lorentzians to the peaks of

the X-ray diffractograms. For this purpose, the (101) reflex of the tetragonal phase and the (-111) reflex of the monoclinic phase were used. In the case of mixed phases, Lorentzians were fitted to both reflexes and additionally to the monoclinic (111) reflex.

$$L = \frac{K\,\lambda}{(w-b)\,\cos\theta_0}\frac{180°}{\pi} \quad (1)$$

In Eq. 1, L is the crystallite size, K the dimensionless shape factor (K = 1), λ is the wavelength of the radiation (Cu-K_α, 0.154 nm), w is the measured FWHM (in deg), b is the instrumental broadening (b = 0.06°), and θ_0 is the Bragg angle.[3] Due to instrumental broadening the method provides reliable data as long as the determined crystallite sizes are below ~80 nm.

The polycrystalline character of the zirconia cores of ZrO_2@SiO_2 particles was also observed in bright field (BF) TEM images. Fig. S7 presents the BF-TEM images of FIB-prepared cross-sectional lamellae of ZrO_2@SiO_2 core-shell particles after calcination at 450, 800, and 1000 °C. The FIB lamellae were prepared with a FEI Helios G3 UC per standard liftout technique and transferred to a copper liftout grid. The final lamellae thicknesses were <100 nm. At larger magnifications, numerous lattice fringes are observed, clearly confirming the polycrystalline nature of the zirconia cores. However, in case of the particle calcined at 450 °C the TEM image also indicates amorphous material. After heating to 800 and 1000 °C the crystallinity increased significantly.

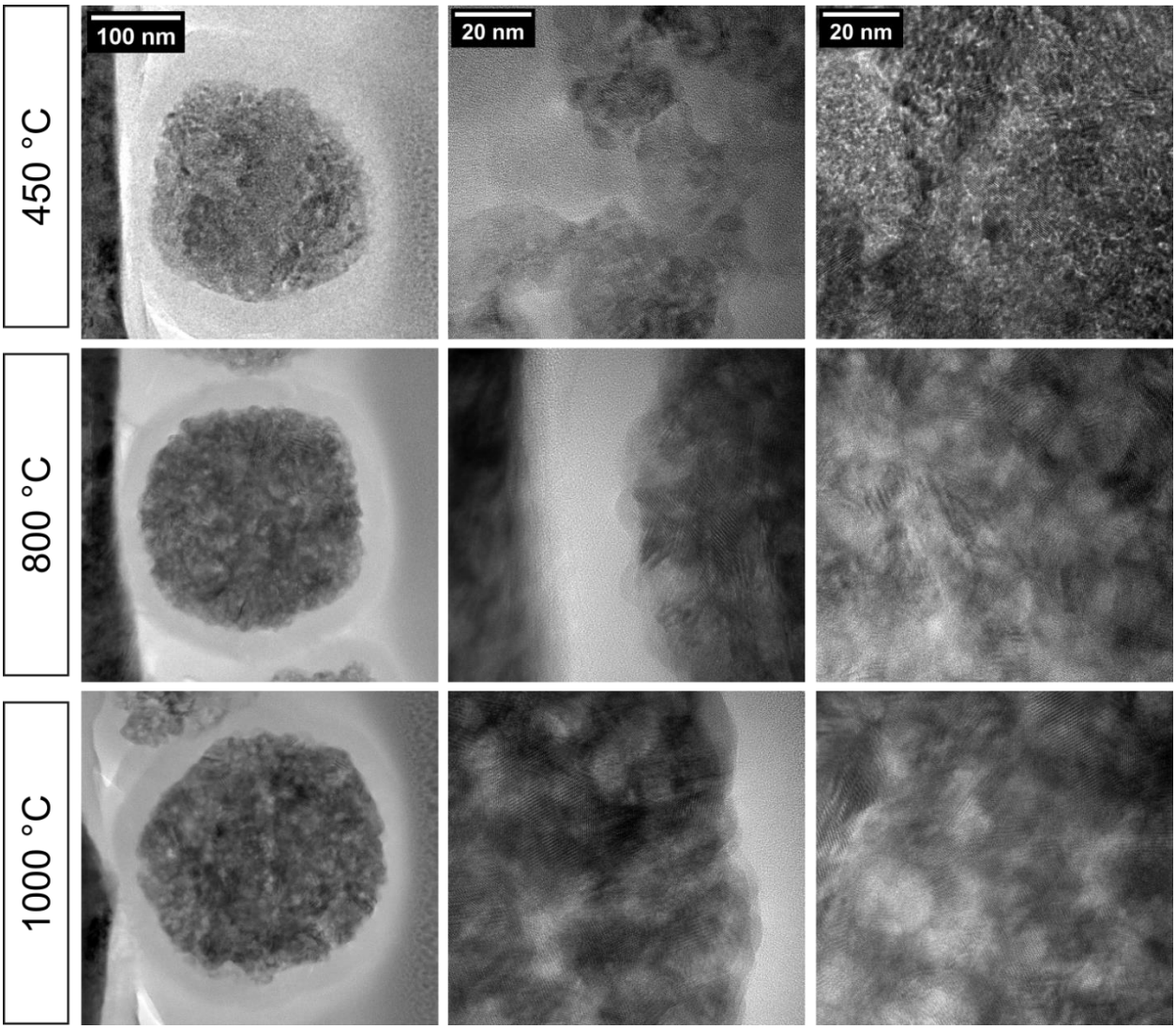

Fig. S7. Bright field (BF) TEM images of cross-sectional FIB lamellae prepared from ZrO_2@SiO_2 core-shell particles (initial shell thickness: ~38 nm) after calcination at different temperatures, as indicated.

Fig. S8 shows another set of HRTEM images of lamellae prepared by FIB technique from the ZrO_2@SiO_2 core-shell particles (initial silica shell thickness: 38 nm) after calcination at 450, 800, and 1000 °C. After 450 °C, the core-shell particles are nanocrystalline, but the zirconia phase still exhibits amorphous material. At the core/shell interface, the amorphous silica phase seems to form close conformal contact to the surface of the zirconia crystallites, however, a clear demarcation is impossible. After heating to higher temperatures, the single crystalline ZrO_2-domains can be

clearly distinguished from the amorphous silica shell and a conformal contact of the two materials at the core/shell interface is clearly recognized.

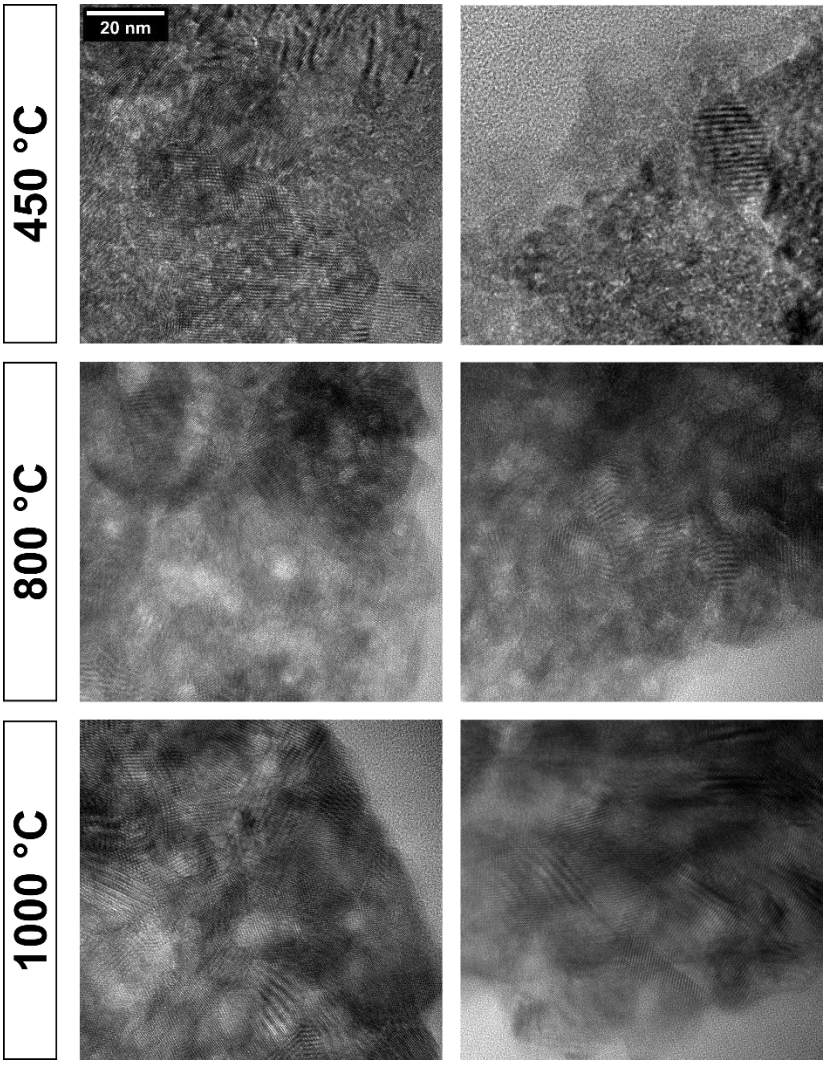

Fig. S8. HRTEM images of cross-sectional FIB lamellae at the core/shell interface prepared from ZrO_2@SiO_2 core-shell particles (initial shell thickness: ~38 nm) after calcination at different temperatures, as indicated.

2.5. EDX mapping

The elemental composition of the ZrO_2@SiO_2 core-shell particles was analyzed via energy dispersive X-ray spectroscopy (EDX). For this purpose, the FIB-prepared lamellae of the core-shell particles (see above) were used. EDX mapping and high angle annular dark-field scanning transmission electron microscopy (HAADF-STEM) imaging was performed using a Talos F200X FEG/TEM (FEI) operated at 200 kV. Fig. S9 shows the EDX maps of ZrO_2@SiO_2 core-shell particles (initial shell thickness: ~38 nm) after calcination at different temperatures. Numerical results of the elemental composition (O, Si, Zr), representing integral values sampled over a specific area of the zirconia core, as indicated in Figure S9, are presented in Tab. S1.

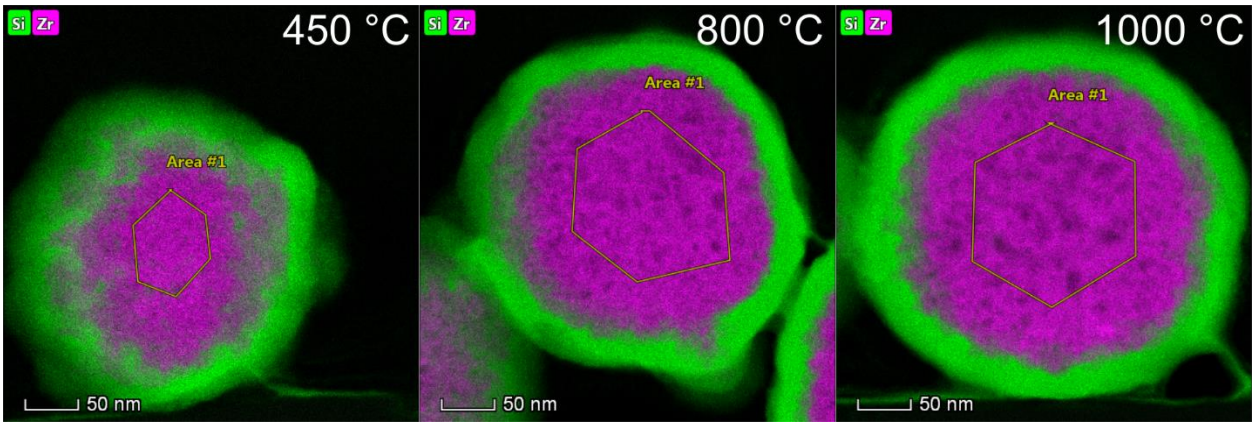

Fig. S9. EDX mappings of FIB lamellae of ZrO_2@SiO_2 core-shell particles (initial shell thickness: ~38 nm; Zr: magenta; Si: green). The FIB lamellae were prepared from core-shell particles calcined at 450, 800, and 1000 °C, as indicated.

Tab. S1. Elemental composition (O, Si, Zr) of zirconia cores of ZrO_2@SiO_2 particles (initial shell thickness: ~38 nm) after calcination at different temperatures, as indicated. The tabulated values were obtained from EDX mappings of FIB-prepared lamellae by integrating the EDX signals over specific areas, as indicated in Fig. S9.

Temperature (°C)	Element	Family	Atomic Fraction (%)	Atomic Error (%)	Mass Fraction (%)	Mass Error (%)	Fit Error (%)
450	O	K	71.38	9.04	31.60	2.74	1.51
450	Si	K	2.20	0.51	1.71	0.36	1.45
450	Zr	K	26.42	4.73	66.69	10.23	0.18
800	O	K	72.88	8.99	32.93	2.77	0.44
800	Si	K	1.57	0.36	1.24	0.26	3.26
800	Zr	K	25.55	4.53	65.82	10.05	0.05
1000	O	K	69.56	9.00	29.65	2.60	0.46
1000	Si	K	2.15	0.50.	1.61	0.34	2.43
1000	Zr	K	28.28	5.14	68.74	10.64	0.06

3. REFERENCES

1 M. Picquart, T. López, R. Gómez, E. Torres, A. Moreno and J. Garcia, *J. Therm. Anal. Calorim.*, 2004, **76**, 755–761.

2 R. C. Garvie and M. F. Goss, *J. Mater. Sci.*, 1986, **21**, 1253–1257.

3 J. I. Langford and A. J. C. Wilson, *J. Appl. Crystallogr.*, 1978, **11**, 102–113.